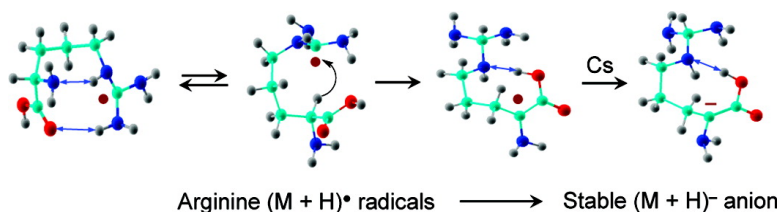


Experimental Evidence for an Inverse Hydrogen Migration in Arginine Radicals

Shigeo Hayakawa, Hiroshi Matsubara, Subhasis Panja, Preben Hvelplund, Steen Brøndsted Nielsen, Xiaohong Chen, and František Tureček

J. Am. Chem. Soc., **2008**, 130 (24), 7645-7654 • DOI: 10.1021/ja800207x • Publication Date (Web): 15 May 2008

Downloaded from <http://pubs.acs.org> on February 8, 2009



More About This Article

Additional resources and features associated with this article are available within the HTML version:

- Supporting Information
- Links to the 1 articles that cite this article, as of the time of this article download
- Access to high resolution figures
- Links to articles and content related to this article
- Copyright permission to reproduce figures and/or text from this article

[View the Full Text HTML](#)

Experimental Evidence for an Inverse Hydrogen Migration in Arginine Radicals

Shigeo Hayakawa,[†] Hiroshi Matsubara,[†] Subhasis Panja,[‡] Preben Hvelplund,[‡] Steen Brøndsted Nielsen,[‡] Xiaohong Chen,[§] and František Tureček^{*,§}

Department of Chemistry, Graduate School of Science, Osaka Prefecture University, Osaka, Japan, Department of Physics and Astronomy, University of Aarhus, DK-8000, Aarhus, Denmark, Department of Chemistry, Bagley Hall, Box 351700, University of Washington, Seattle, Washington 98195-1700

Received January 9, 2008; E-mail: turecek@chem.washington.edu

Abstract: Radicals formed by electron transfer to protonated arginine have been predicted by theory to undergo an inverse migration of the hydrogen atom from the C_α position to the guanidine carbon atom. Experiments are reported here that confirm that a fraction of arginine and arginine amide radicals undergo such an inverse hydrogen migration. The rearranged arginine and arginine amide C_α radicals are detected as stable anions after charge inversion by collisions with Cs atoms of precursor cations at 3 and 50 keV kinetic energies. RRKM calculations on the B3-PMP2/aug-cc-pVTZ potential energy surface indicate that arginine radicals undergo rapid rotations of the side chain to reach conformations suitable for C_α-H transfer, which is calculated to be fast ($k > 10^9 \text{ s}^{-1}$) in radicals formed by electron transfer. By contrast, H-atom transfer from the guanidine group onto the carboxyl or amide C=O groups is >50 times slower than the C_α-H atom migration. The guanidine group in arginine radicals is predicted to be a poor hydrogen-atom donor but a good H-atom acceptor and thus can be viewed as a radical trap. This property can explain the frequent observation of nondissociating cation radicals in electron capture and electron transfer mass spectra of arginine-containing peptides.

Introduction

One-electron reduction of protonated guanidinium cations forms transient radicals in which the unpaired electron is delocalized over the guanidinium group.¹ Guanidine is a side-chain functionality in arginine, the most basic natural amino acid, whose residue is likely to be protonated in peptide and protein cations in solution at pH <12 and in the gas phase, forming guanidinium cations.² Reduction by electron capture or transfer of arginine guanidinium groups in multiply protonated gas-phase peptide or protein ions produces guanidinium radicals that have been considered as hydrogen atom donors for intramolecular transfer to the peptide backbone.³ Such transfer could trigger backbone N-C_α bond cleavages, producing N- and C-terminal fragment ions that are observed in electron capture and electron transfer dissociation spectra (abbreviated as ECD and ETD, respectively) and used for peptide sequencing by mass spectrometry.⁴ In addition to its propensity for protonation, the significance of arginine is

underlined by its frequent occurrence as a C-terminal residue in tryptic peptides that are commonly used in proteomics.

The properties of arginine (Arg) residues in ECD and ETD of peptide ions have been studied and some interesting features have been noted. For example, peptides having Arg residues at the C-terminus often, albeit not always, give a fraction of stable cation radicals upon electron capture⁵ or transfer (Scheme 1).⁶

In the presence of Arg residues at both peptide termini, the protonated C-terminus undergoes preferential reduction upon electron capture, as judged from the prevalence of ion fragments that carry the remaining charge on the N-terminal Arg residue.^{5c,6,7}

It has been shown recently that arginine amide radicals, when formed by femtosecond electron transfer to protonated arginine amide, did not undergo facile hydrogen atom migration from the guanidinium group onto the amide carbonyl.⁸ Instead, the radicals dissociated by loss of neutral guanidine, which is a common dissociation of arginine-containing peptide ions on ECD and ETD, as well. Ab initio calculations on arginine amide radicals indicated that migration of a guanidinium hydrogen

[†] Osaka Prefecture University.

[‡] University of Aarhus.

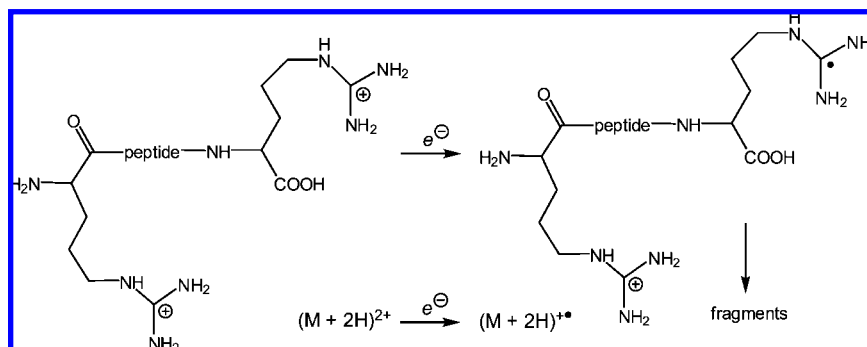
[§] University of Washington.

- (1) Hao, C.; Seymour, J. L.; Tureček, F. *J. Phys. Chem. A* **2007**, *112*, 8829–8843.
- (2) (a) Harrison, A. G. *Mass Spectrom. Rev.* **1997**, *16*, 201–217. (b) Bleiholder, C.; Suhai, S.; Paizs, B. *J. Am. Soc. Mass Spectrom.* **2006**, *17*, 1275–1281.
- (3) (a) Zubarev, R. A.; Kelleher, N. L.; McLafferty, F. W. *J. Am. Chem. Soc.* **1998**, *120*, 3265–3266. (b) Zubarev, R. A.; Horn, D. M.; Fridriksson, E. K.; Kelleher, N. L.; Kruger, N. A.; Lewis, M. A.; Carpenter, B. K.; McLafferty, F. W. *Anal. Chem.* **2000**, *72*, 563–573.

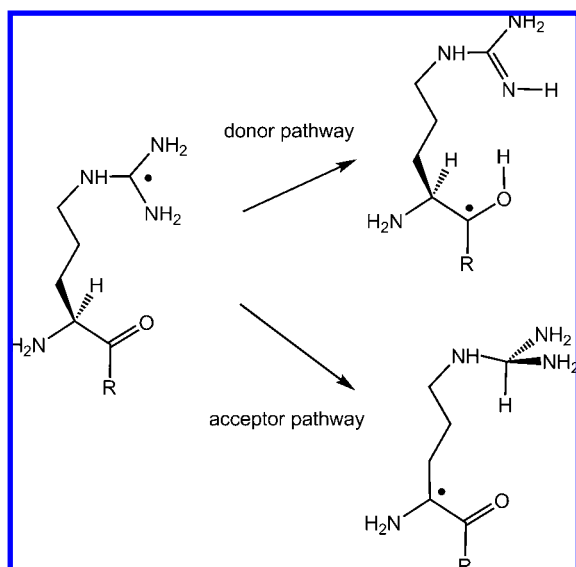
- (4) Cooper, H. J.; Hakansson, K.; Marshall, A. G. *Mass Spectrom. Rev.* **2005**, *24*, 201–222.

- (5) (a) Cooper, H. J.; Hudgins, R. R.; Hakansson, K.; Marshall, A. G. *J. Am. Soc. Mass Spectrom.* **2002**, *13*, 241–249. (b) Cooper, H. J. *J. Am. Soc. Mass Spectrom.* **2005**, *16*, 1932–1940. (c) Fung, Y. M. E.; Duan, L.; Chan, T. W. D. *Eur. J. Mass Spectrom.* **2004**, *10*, 449–457.
- (6) Xia, Y.; Gunawardena, H. P.; Erickson, D. E.; McLuckey, S. A. *J. Am. Chem. Soc.* **2007**, *129*, 12232–12243.
- (7) Fung, Y. M. E.; Chan, T. W. D. *J. Am. Soc. Mass Spectrom.* **2005**, *16*, 1523–1535.
- (8) Chen, X.; Tureček, F. *J. Am. Chem. Soc.* **2006**, *128*, 12520–12530.

Scheme 1



Scheme 2



atom onto the amide carbonyl forming a ketyl radical (donor pathway, Scheme 2) required a higher transition-state energy than the inverse migration of the C_{α} -hydrogen atom onto the guanidinium carbon atom (acceptor pathway, Scheme 2) forming a C_{α} radical intermediate. However, since both intermediates were isobaric with the reactant, they could not be distinguished by mass spectrometry after conversion to cations. We now report a joint experimental and computational study of transient radicals that provides unequivocal evidence for the acceptor pathway in arginine and arginine amide radicals produced by collisional electron transfer in the gas phase.

Experimental Section

Materials and Methods. Charge inversion mass spectra were measured on sector instruments at the University of Aarhus, Denmark, and at the Osaka Prefecture University, Japan. Both instruments have been described in detail.^{9,10} The Osaka instrument comprises a double-focusing mass spectrometer (Hitachi M80B) as MS-I to mass separate precursor ions, a 4 cm long collision cell, and a toroidal electrostatic analyzer having a 216 mm central radius as MS-II to mass-analyze secondary ions.⁹ Measurements on the Aarhus instrument used arginine (Sigma–Aldrich) that was electrosprayed from 50/50 aqueous methanol solution at 1 mM

concentration, and the ions were accelerated to 50 keV kinetic energy. Protonated arginine ions, $(\text{Arg} + \text{H})^+$, at m/z 175 were mass-selected by a large-scale magnetic sector and focused onto a special collision cell maintained at 107–120 °C that contained cesium vapor at pressures allowing double collisions with the fast beam. Anions from charge inversion were analyzed by a hemispherical electrostatic analyzer to provide charge-reversal ($^+\text{CR}^-$) mass spectra.¹¹ $^+\text{CR}^-$ mass spectra were also obtained for $(\text{Arg}-d_7 + \text{D})^+$ which was obtained by electrospraying arginine from $\text{CH}_3\text{OD}/\text{D}_2\text{O}$ while saturating the ionizer space with D_2O vapor. Multiple scans were taken and summed to obtain sufficient ion counts for good quality spectra. Measurements on the Osaka instrument used liquid secondary-ion mass spectrometry (LSIMS) with glycerol as a matrix to produce $(\text{Arg} + \text{H})^+$ and protonated arginine amide, $(\text{ArgNH}_2 + \text{H})^+$, ions in the gas phase. The ions were accelerated to 3 kV, mass-selected, and converted to anions by multiple collisions with Cs vapor in a special high-temperature collision cell. Anions from charge inversion were analyzed by a toroidal electrostatic analyzer to provide $^+\text{CR}^-$ mass spectra.⁹ The anion lifetimes, defined as the ion drift time from the charge-inversion collision cell to the detector, were 6 and 13 μs on the Aarhus and Osaka instruments, respectively.

Calculations. Standard ab initio and density functional theory calculations were performed with the Gaussian 03 suite of programs.¹² Geometries were optimized with B3LYP¹³ and the 6-31+G(d,p) basis set. The 6-31++G(d,p) basis set was used for open-shell systems (radicals and cation radicals). Tables of complete optimized structures are available as Supporting Information. Local energy minima and transition states were characterized by harmonic frequency analysis to have the appropriate number of imaginary frequencies (zero for local minima and one for transition states). Improved energies were obtained by single-point calculations on the B3LYP-optimized geometries. The single-point calculations used B3LYP and Møller–Plesset perturbation theory truncated at second order with valence-electrons-only excitations [MP2(frozen core)] and basis sets of triple- ζ quality that were furnished with multiple shells of polarization and diffuse functions, such as 6-311++G(2d,p), 6-311++G(3df,2p), and aug-cc-pVTZ.¹⁴ For the molecular systems of the arginine radical size these basis sets comprised 639, 876, and 1281 primitive gaussians, respectively.

(9) (a) Hayakawa, S. *Int. J. Mass Spectrom.* **2001**, *212*, 229–247. (b) Hayakawa, S.; Kabuki, N.; Kawamura, Y.; Kitaguchi, A. *J. Mass Spectrom. Soc. Jpn.* **2005**, *53*, 33–51. (c) Hayakawa, S. *J. Mass Spectrom.* **2004**, *39*, 111–135. (d) Hayakawa, S.; Kabuki, N. *Eur. Phys. J. D* **2006**, *38*, 163–176.

(10) (a) Boltalina, O. V.; Hvelplund, P.; Jørgensen, T. J. D.; Larsen, M. C.; Larsson, M. O.; Sharoitchenko, D. A.; Sørensen, M. *Phys. Rev. A* **2000**, *62*, 023202. (b) Larsson, M. O.; Hvelplund, P.; Larsen, M. C.; Shen, H.; Cederquist, H.; Schmidt, H. T. *Int. J. Mass Spectrom.* **1998**, *177*, 51–62. (11) (a) Hvelplund, P.; Liu, B.; Nielsen, S. B.; Tomita, T. S., *Int. J. Mass Spectrom.* **2003**, *225*, 83–87. (b) Hvelplund, P.; Liu, B.; Nielsen, S. B.; Panja, S.; Pouilly, J.-C.; Stochkel, K. *Int. J. Mass Spectrom.* **2007**, *263*, 66–70. (12) Frisch, M. J., et al. *Gaussian 03*, Revision B.05; Gaussian, Inc.: Pittsburgh, PA, 2003. (13) (a) Becke, A. D. *J. Chem. Phys.* **1993**, *98*, 1372–1377. (b) Becke, A. D. *J. Chem. Phys.* **1993**, *98*, 5648–5652. (c) Stephens, P. J.; Devlin, F. J.; Chabalowski, C. F.; Frisch, M. J. *J. Phys. Chem.* **1994**, *98*, 11623–11627.

Spin-unrestricted formalism was used for calculations of open-shell systems. Contamination by higher spin states was modest, as judged from the expectation values of the spin operator $\langle S^2 \rangle$ that were ≤ 0.76 for UB3LYP and ≤ 0.78 for UMP2 calculations for most radicals. The UMP2 energies were corrected by spin annihilation¹⁵ that reduced $\langle S^2 \rangle$ to close to the theoretical value for a pure doublet state (0.75). The single-point B3LYP and spin-projected MP2 energies were averaged according to the B3-PMP2 procedure¹⁶ that results in cancellation of small errors inherent to both approximations and provides dissociation and transition-state energies of improved accuracy, as has been previously shown for a number of closed-shell and open-shell systems.¹⁷ Atomic spin and charge densities were calculated by the natural population analysis (NPA) method.¹⁸

Unimolecular rate constants were calculated by the Rice–Ramsperger–Kassel–Marcus (RRKM)¹⁹ theory using Hase’s program²⁰ that was recompiled in C++ and run under Windows XP.²¹ The RRKM rate constants were obtained by direct count of quantum states at internal energies that were increased in 2 kJ mol⁻¹ steps from the transition state up to 400 kJ mol⁻¹ above the reactant. Rotations were treated adiabatically, and the calculated $k(E, J, K)$ microscopic rate constants were Boltzmann-averaged over the thermal distribution of rotational states at 298 K, corresponding to the electrospray ion source temperature, to provide $k(E)$.

Results and Discussion

Charge inversion with Cs of (Arg + H)⁺ ions resulted in substantial dissociation by loss of H₂ (m/z 173), ammonia (m/z 158), CO₂ (m/z 131), and guanidine (m/z 116), in addition to the formation of small anions at m/z 42, 41, and 26 (Figure 1). Interestingly, the ⁺CR⁻ spectra showed a peak of an (Arg + H)⁻ anion at m/z 175. The relative intensities of (Arg + H)⁻ and its fragments differed for the two beam instruments. In particular, the ⁺CR⁻ spectrum obtained with electrospray produced cations and at shorter anion lifetimes showed a substantially higher fraction of (Arg + H)⁻ and much less dissociation by loss of H₂ (Figure 1b) than did the spectrum in Figure 1a. An intense peak of a nondissociating anion was also obtained for (Arg-*d*₇ + D)⁻ that appeared at m/z 183 (Figure 1b,d). The identity of the (Arg + H)⁻ ion is corroborated by its m/z ratio, mass shift upon isotope exchange, and the beam profile, which is similar to that of the cation precursor (Figure 1a,c). The last finding shows that the formation of the surviving anions did not involve kinetic energy release, which would be expected for a fragment. Thus, the ⁺CR⁻ spectra indicated that fractions of stable (Arg + H)⁻ anions were formed upon charge inversion.

It is worth noting that transfer of two electrons in (Arg + H)⁺ → (Arg + H)⁻ most likely occurs in two sequential

collisions with Cs atoms, the first neutralizing the cation to an (Arg + H)^{*} radical, which acquires an additional electron upon a second collision with another Cs atom.^{9c,d} Thus, the fact that nondissociating anions were observed is also evidence for a fraction of nondissociating (Arg + H)^{*} radicals. The lifetime of the radicals to be ionized to anions is limited from above by their residence time in the collision cell and the Poisson distribution of collisions with Cs atoms. For 50 keV particles of a 2.35×10^5 m s⁻¹ velocity, the residence time in a 4-cm cell is limited to 170 ns. Due to sequential collisions, the probability for conversion to anions is given by eq 1, where I_{anion} and I_{cation} are the anion and precursor cation currents, respectively; σ_n and σ_- are the collision cross sections for $A^+ \rightarrow A$ and $A \rightarrow A^-$, respectively; N is the cesium atom number density, L is the cell length, and l is the path length for the precursor cation undergoing the first charge-transfer collision in the cell.

$$\frac{I_{\text{anion}}}{I_{\text{cation}}} = (1 - e^{-N\sigma_n l})(1 - e^{-N\sigma_-(L-l)}) \approx N^2 \sigma_n \sigma_-(L-l)l \quad (1)$$

For Cs atom number densities corresponding to the experimental temperature (1.2×10^{13} atoms/cm³ at 383 K), eq 1 has a maximum at $l = L/2$, indicating that anions are most likely to be formed in the second half of the cell. This gives the most probable neutral lifetime as $170/2 = 85$ ns for (Arg + H)^{*} radicals that are converted to anions and detected in the ⁺CR⁻ spectrum. Lifetime considerations are important for kinetic analysis of neutral unimolecular reactions, as addressed below.

⁺CR⁻ of arginine amide cations, (ArgNH₂ + H)⁺, at 3 keV (Figure 2) showed substantial dissociation by loss of H₂ (m/z 172), ammonia (m/z 157), CH₃N₂ (m/z 130), and guanidine (m/z 115) and formation of small mass fragments. However, a small fraction of nondissociating anions was observed that was produced from (ArgNH₂ + H)^{*} radicals. This observation is consistent with the previous detection of nondissociating (ArgNH₂ + H)^{*} radicals upon collisional neutralization with dimethyldisulfide followed by ionization to cations.⁸

Ion and Radical Structures and Dissociation Energetics. In order to interpret the ⁺CR⁻ data for (Arg + H)⁺ and (ArgNH₂ + H)⁺, we analyzed with B3LYP calculations the structures of the precursor cations, radical intermediates, and anions. Relative energies were then obtained by single-point calculations that combined B3LYP and MP2 calculations with increasingly larger basis sets up to B3-PMP2/aug-cc-pVTZ. Anion detection on the 6–13 μs time scale of the present experiments is possible only for bound species, so that the respective radical precursors must have positive electron affinities, which provide the main criterion for the selection of plausible structures for the anions observed experimentally.

The global minimum for (Arg + H)⁺ conformers is represented by structure **1a**⁺, which shows two hydrogen bonds between the protonated guanidinium group and the NH₂ and COOH neutral groups (Figure 3), as also established by several previous studies.²² Other (Arg + H)⁺ conformers, for example, **1b**⁺ and **1c**⁺, were found to be substantially less stable than **1a**⁺, and their calculated $\Delta H_{\text{g},298}^\circ$ and $\Delta G_{\text{g},298}^\circ$ values (Table 1) indicate that they cannot be expected to be significantly (<1%) populated in a gas-phase equilibrium at 298 K. (ArgNH₂ + H)⁺ cations (Figure 3) show a similar order of relative energies, with the doubly H-bonded conformer **2a**⁺ being the most stable structure, while the other H-bonded structures **2b**⁺ and **2c**⁺ are 10–37 kJ mol⁻¹ less stable ($\Delta G_{\text{g},298}^\circ$, Table 1).

- (14) Dunning, T. H. *J. Chem. Phys.* **1989**, *90*, 1007–1023.
 (15) (a) Schlegel, H. B. *J. Chem. Phys.* **1986**, *84*, 4530–4534. (b) Mayer, I. *Adv. Quantum Chem.* **1980**, *12*, 189–262.
 (16) Tureček, F. *J. Phys. Chem. A* **1998**, *102*, 4703–4713.
 (17) (a) Tureček, F.; Polášek, M.; Frank, A. J.; Sadílek, M. *J. Am. Chem. Soc.* **2000**, *122*, 2361–2370. (b) Polášek, M.; Tureček, F.; *J. Am. Chem. Soc.* **2000**, *122*, 9511–9524. (c) Tureček, F.; Yao, C. *J. Phys. Chem. A* **2003**, *107*, 9221–9231. (d) Rablen, P. R. *J. Am. Chem. Soc.* **2000**, *122*, 357–368. (e) Rablen, P. R. *J. Org. Chem.* **2000**, *65*, 7930–7937. (f) Rablen, P. R.; Bentrup, K. H. *J. Am. Chem. Soc.* **2003**, *125*, 2142–2147. (g) Hirama, M.; Tokosumi, T.; Ishida, T.; Aihara, J. *J. Chem. Phys.* **2004**, *305*, 307–316.
 (18) Reed, A. E.; Weinstock, R. B.; Weinhold, F. *J. Chem. Phys.* **1985**, *83*, 735–745.
 (19) Gilbert, R. G.; Smith, S. C. *Theory of Unimolecular and Recombination Reactions*; Blackwell Scientific Publications: Oxford, U.K., 1990; pp 52–132.
 (20) Zhu, L.; Hase, W. L. *Quantum Chemistry Program Exchange*; Indiana University: Bloomington, IN, 1994; program QCPE 644.
 (21) Frank, A. J.; Sadílek, M.; Ferrier, J. G.; Tureček, F. *J. Am. Chem. Soc.* **1997**, *119*, 12343–12353.

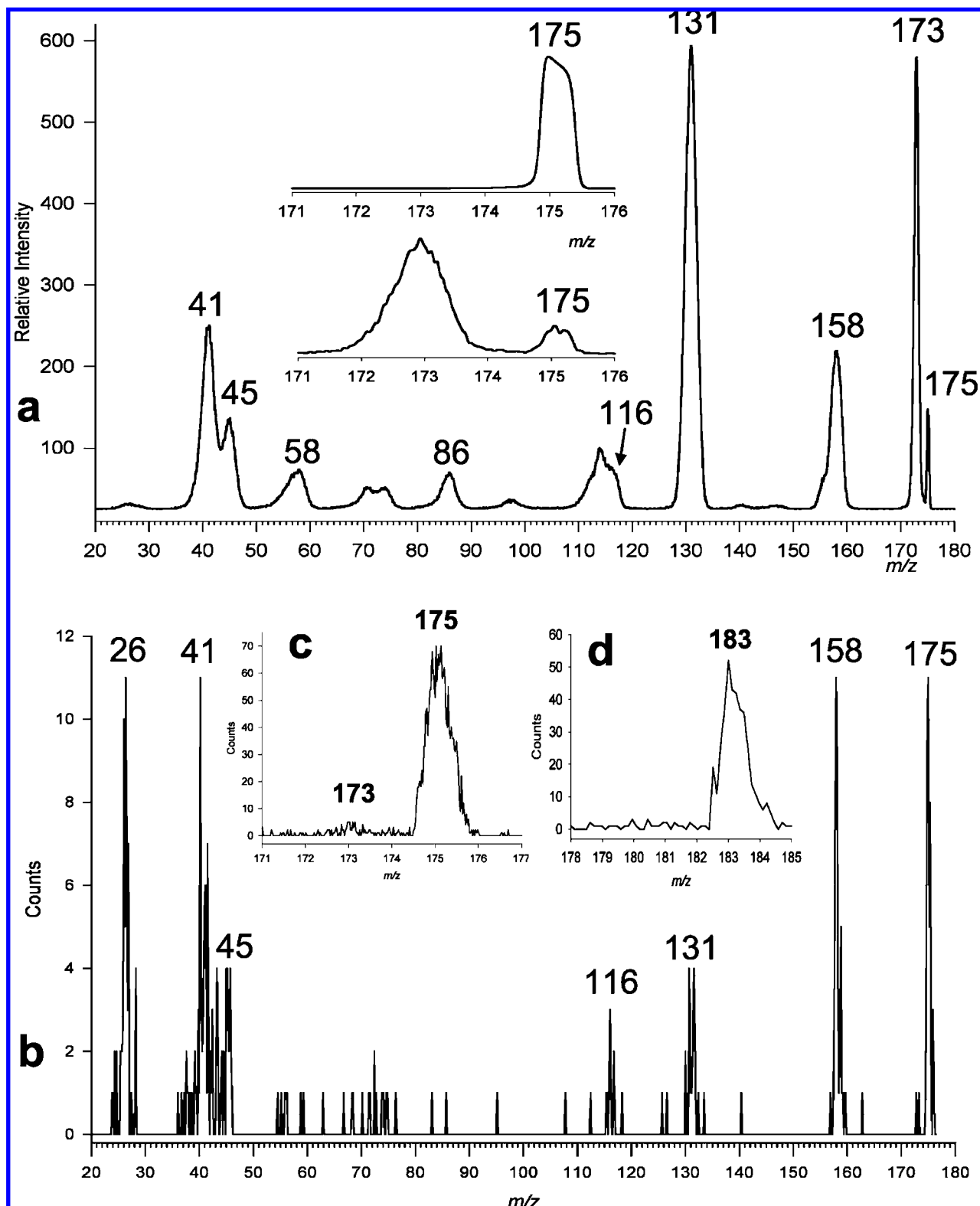


Figure 1. $^{+}CR^{-}$ mass spectra of $(Arg + H)^{+}$ cations with Cs as a target. (a) $^{+}CR^{-}$ mass spectrum measured at 3 keV on the Osaka instrument. Insets show (top) main beam profile and (bottom) m/z 175 region with the survivor anion. (b) $^{+}CR^{-}$ mass spectrum measured at 50 keV on the Aarhus instrument. (c) m/z 175 survivor anion profile measured with a narrow energy-analyzer entrance slit and increased mass resolution. (d) m/z 183 survivor anion from $(Arg-d_1 + D)^{+}$ measured with a narrow energy analyzer entrance slit.

Electron attachment to $\mathbf{1a}^{+}$ results in an $(Arg + H)^{\bullet}$ radical ($\mathbf{1a}$), which is a local energy minimum. The recombination energy (RE) for $\mathbf{1a}^{+} \rightarrow \mathbf{1a}$ shows a large difference between the adiabatic value, $RE_{\text{adiab}} = 3.39$ eV, and the vertical value, $RE_{\text{vert}} = 2.19$ eV (Table 2). Both the adiabatic and vertical

recombination energies are lower than the ionization energy of the Cs electron donor ($IE = 3.894$ eV), indicating that the collisional electron transfer to $\mathbf{1a}^{+}$ is endothermic. In such a case, the mean internal energy of the radical $\mathbf{1a}$ formed, $\langle E_{\text{int}} \rangle$, can be approximated²³ by eq 2, where E_{ion} is the precursor ion

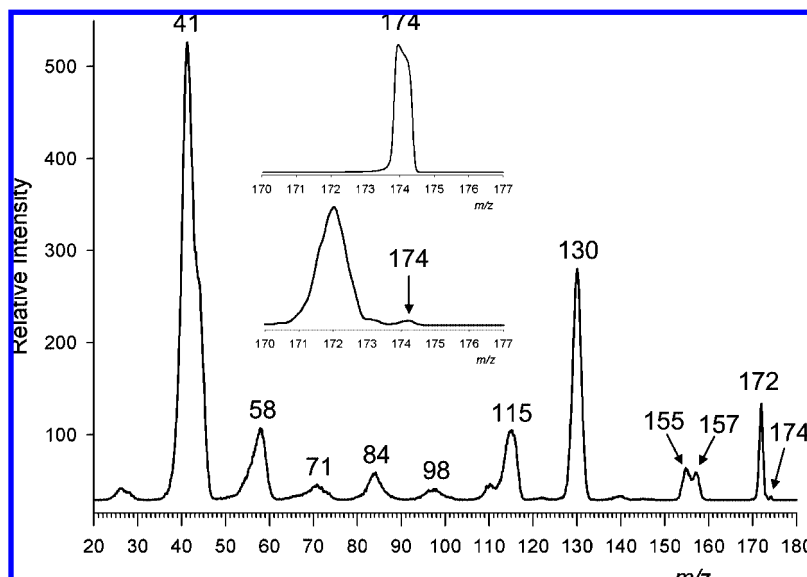


Figure 2. $^+CR^-$ mass spectra of $(\text{ArgNH}_2 + \text{H})^+$ cations with K as a target. Insets show (top) main beam profile and (bottom) m/z 174 region with the survivor anion.

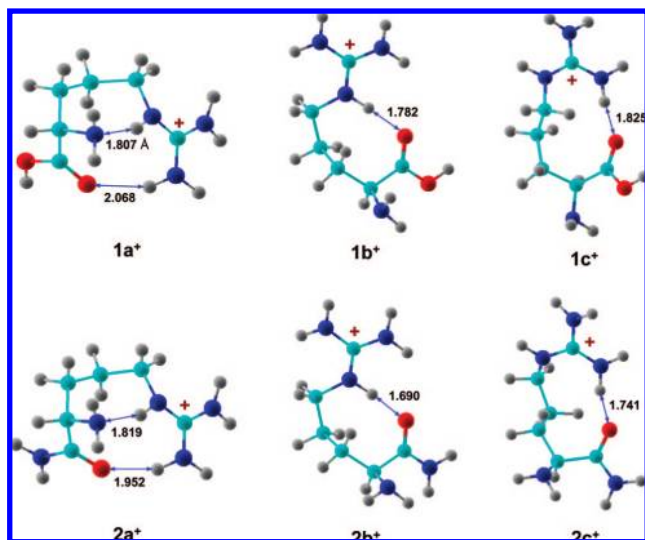


Figure 3. B3LYP/6-31+G(d,p) optimized structures of $(\text{Arg} + \text{H})^+$ cations $1a^+ - 1c^+$ and $(\text{ArgNH}_2 + \text{H})^+$ cations $2a^+ - 2c^+$. Intramolecular hydrogen bonds are indicated by blue double-headed arrows, and the distances are given in angstroms.

Table 1. Relative Energies of Arginine Cations

ion	relative energy ^{a,b}			
	B3LYP 6-31+G(d,p)	B3-MP2		
	6-31+G(d,p)	6-311++G(2d,p)	6-311++G(3df,2p)	aug-cc-pVTZ
$1a^+$	0	0	0	0
$1b^+$	23	25	22	22 (14) ^c
$1c^+$	31	33	31	30 (23) ^c
$2a^+$	0	0	0	0
$2b^+$	23	22	20	19 (10) ^c
$2c^+$	42	43	41	41 (37) ^c

^a In units of kilojoules per mole. ^b Including B3LYP/6-31+G(d,p) zero-point energies and enthalpies and referring to 298 K. ^c Relative $\Delta G_{g,298}^\circ$ values.

rovibrational enthalpy (33 kJ mol⁻¹ at 298 K) and E_{FC} is the vibrational excitation due to Franck–Condon effects ($E_{FC} \approx 104$ kJ mol⁻¹), giving $\langle E_{int} \rangle(1a) \approx 137$ kJ mol⁻¹.

Table 2. Cation Recombination Energies and Radical Electron Affinities

species	recombination energy ^a /electron affinity ^b	
	vertical ^c	adiabatic ^c
$1a^+$	2.14 (2.19) ^d	3.40 (3.37) ^d (3.39) ^e
$1b^+$	2.70 (2.71) ^d (2.75) ^e	
$1c^+$	2.78 (2.79) ^d (2.82) ^e	3.61 (3.57) ^d (3.59) ^e
$2a^+$	2.46 (2.47) ^d	3.22 (3.20) ^d (3.22) ^e
$2b^+$	2.52 (2.53) ^d	3.29 (3.22) ^d (3.25) ^e
$2c^+$	2.44 (2.67) ^d (2.71) ^e	3.53 (3.50) ^d (3.51) ^e
$1a$	-0.45	
$1c$	-0.53	
$1d$	-0.81 (-0.76) ^d	
$1g$	-0.42 (-0.37) ^d	
$1i$	0.41 (0.47) ^d	1.12 (1.13) ^d
$1j$	0.27 (0.32) ^d (0.37) ^e	0.98 (1.00) ^d (1.03) ^e
$2f$	0.51 (0.57) ^d	1.35 (1.36) ^d
4	0.22 (0.28) ^d	0.93 (0.94) ^d

^a $-\Delta H_{g,0}^\circ$ for electron attachment in cations from B3-PMP2/6-311++G(2d,p) single-point energy calculations. Adiabatic recombination energies include zero-point corrections. ^b $-\Delta H_{g,0}^\circ$ for electron attachment in radicals from B3-PMP2/6-311++G(2d,p) single-point energy calculations. Adiabatic electron affinities include zero-point corrections. ^c All values are given in electronvolts ^d From B3-PMP2/6-311++G(3df,2p) single-point energy calculations. ^e From B3-PMP2/aug-cc-pVTZ single-point energy calculations.

$$\langle E_{int} \rangle = E_{ion} + E_{FC} \quad (2)$$

The Franck–Condon effects stem from the different equilibrium geometries of $1a^+$ and $1a$. In particular, the ion shows a planar guanidinium group whereas the same group in the radical is pyramidal at the C atom. Other substantial differences are in the guanidinium C–N bond lengths, which are 1.328–1.349

- (22) (a) Rak, J.; Skurski, P.; Simons, J.; Gutowski, M. *J. Am. Chem. Soc.* **2001**, *123*, 11695–11707. (b) Csonka, I. P.; Paizs, B.; Suhai, S. *J. Mass Spectrom.* **2004**, *39*, 1025–1035. (c) Shek, P. Y. I.; Zhao, J.; Ke, Y.; Siu, K. W. M.; Hopkinson, A. C. *J. Phys. Chem. A* **2006**, *110*, 8262–8296. (d) Ling, S.; Yu, W.; Huang, Z.; Lin, Z.; Haranczyk, M.; Gutowski, M. *J. Phys. Chem. A* **2006**, *110*, 12282–12291. (e) Bush, M. F.; O'Brien, J. T.; Prell, J. S.; Saykally, R. J.; Williams, E. R. *J. Am. Chem. Soc.* **2007**, *129*, 1612–1622.
- (23) (a) Wolken, J. K.; Tureček, F. *J. Phys. Chem. A* **1999**, *103*, 6268–6281. (b) Tureček, F. *Int. J. Mass Spectrom.* **2003**, *227*, 327–338.

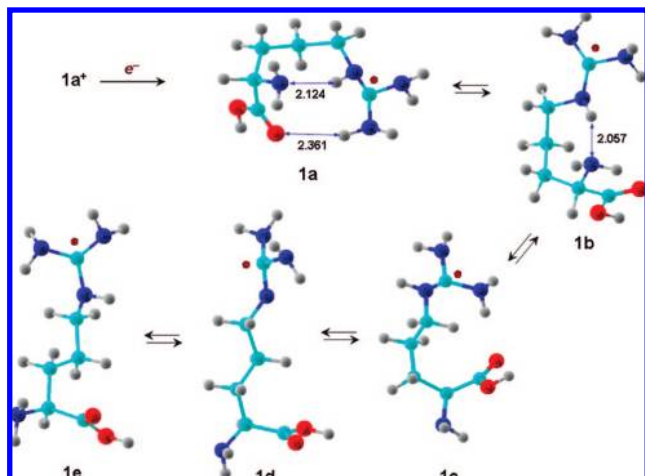


Figure 4. B3LYP/6-31++G(d,p) optimized structures of (Arg + H) radicals **1a**–**1e**. Description as in Figure 3.

Å in **1a**⁺ and 1.410–1.413 Å in **1a**. Similar Franck–Condon effects have been reported for guanidinium¹ and (ArgNH₂ + H)[•] radicals,⁸ and appear to be of general nature for ions of this type. The adiabatic recombination energy of **2a**⁺ was calculated here as $RE_{\text{adiab}} = 3.22$ eV to be compared with $RE_{\text{adiab}} = 3.51$ eV for **2c**⁺.⁸

In contrast to ions **1a**⁺–**1c**⁺, arginine radicals exist as several interconverting conformers of closely similar energies, for example, **1a**–**1e** (Figure 4). A major structural effect of electron attachment besides pyramidization and bond length extension is the substantial weakening of intramolecular hydrogen bonds in the radicals. This manifests itself by the longer H–N and H–O distances in **1a** (Figure 4) and also by the exothermic unfolding to **1d** and **1e**, which lack hydrogen bonds between the guanidinium and carboxyl groups. The radical conformers are interconnected by transition states for rotations about single C–C and C–N bonds. These require very low TS energies: $E_{\text{TS1}} = 11.6$ kJ mol^{−1} for the guanidine group rotation about the C_ε–N bond in **1a**, giving yet another unfolded low-energy conformer **1f** (Table 3, Scheme S1 in Supporting Information). The (ArgNH₂ + H)[•] radicals **2a**–**2e** are quite analogous to **1a**–**1f**. The doubly H-bonded structure **2a** was found to be the most stable conformer compared to **2b**–**2e** (Table 3, Scheme S2 in Supporting Information).

However, arginine radicals of the type represented by structures **1a**–**1f** and **2a**–**2e** were unlikely to have bound states for an additional electron, as documented by the calculated vertical electron affinities that were consistently negative, for example, those for **1a**, **1c**, and **1d** (Table 2). Hence, stable arginine anions must be formed from other radical structures that were produced by unimolecular rearrangements of the guanidinium radicals on the 85 ns time scale of the experiment.

To gain more insight into the nature of arginine radicals, we analyzed the reaction paths for dissociations and isomerizations of **1a** to establish the transition-state energies and to calculate unimolecular rate constants for the competing reactions. Scheme 3 shows optimized transition-state structures for a guanidinium C–N bond dissociation (**TS2**), N–H bond dissociation (**TS3**), and H-atom migration onto the carboxyl group (**TS4**) producing the dihydroxycarbonyl radical **1g**. Also displayed is yet another radical conformer (**1h**) that can be accessed from **1a** through low-energy side-chain rotations analogous to that shown in Scheme S1 in Supporting Information. The relevant dissociation, isomerization, and TS energies are summarized in Table 3.

Loss of Guanidine. Loss of a guanidine molecule from **1a** is a mildly endothermic dissociation that requires only 12 kJ mol^{−1} at the thermochemical threshold to form the 1-amino-1-carboxylbut-4-yl radical (**3**). This dissociation by a C–N bond cleavage has to overcome a 75 kJ mol^{−1} energy barrier in **TS2**. A similar TS energy was calculated for an analogous loss of guanidine from the unfolded conformer **1d** (**TS6**; Scheme 4, Table 2). Since the TS energies for the guanidine C–N bond dissociations do not seem to appreciably depend on the radical reactant conformation, the dissociation can be considered to proceed through multiple pathways involving near-degenerate transition states that differ in their side-chain conformations. We note that a product due to guanidine loss was detected in the CR mass spectrum of (Arg + H)⁺ at *m/z* 116 (Figure 1). However, primary alkyl radicals of the **3** type do not form stable anions,²⁴ and thus the formation of the anion in the spectrum must be preceded by a fast isomerization of **3** to another structure. One such possibility is a highly exothermic migration of the C_α–H in **3** through a low-lying **TS8** to give the more stable C_α radical **4** (Scheme 4). Radical **4** was calculated to have a substantial electron affinity, both vertical (0.22 eV) and adiabatic (0.94 eV, Table 2), to give a stable anion **4**[−] to be detected in the CR spectrum. Loss of guanidine from (ArgNH₂ + H)[•] radicals has been studied previously⁸ and found to be kinetically competitive with the other unimolecular reactions of arginine amide radicals.

Loss of H. Simple guanidinium radicals have been found to lose H atoms from the NH₂ groups to re-form the guanidine moiety.¹ With **1a** and **1d**, the loss of H was calculated to require dissociation energies that were substantially higher than those for the other dissociations and isomerizations of these radicals. Cleavage of guanidinium N–H bonds in **1a** and **1d** involves energy barriers of 91 and 87 kJ mol^{−1} for **TS3** and **TS7**, respectively, which are comparable to the barrier for an analogous N–H bond dissociation in **2c** (87 kJ mol^{−1}).⁸ It should be noted that arginine and arginine amide molecules arising by H atom loss from the respective radicals are unlikely to form stable anions, because neither the guanidine nor the carboxyl or amide groups have positive electron affinities.

N–H→O Migration. Isomerization by N–H→O migration in **1a** was calculated to require a 43 kJ mol^{−1} barrier in **TS4** (Scheme 3, Table 3). However, the dihydroxycarbonyl product (**1g**) was 28 kJ mol^{−1} less stable than **1a**, and if formed, it would undergo a facile reverse isomerization to the more stable isomer **1a**. Furthermore, **1g** is predicted not to form a bound anion, as judged from its calculated negative vertical electron affinity (−0.37 eV, Table 2). Hence, reversible isomerization to **1g** followed by electron transfer cannot account for the formation of stable anions upon CR. An N–H→O migration in **2a** also requires an energy barrier to form aminoketyl radical **2g** (Scheme 5) However, **2g** is 16 kJ mol^{−1} less stable than **2a** and is expected to undergo fast reversible isomerization to the latter structure.

C_α–H→C Migration. The lowest TS energy was found for an exothermic transfer of the hydrogen atom from C_α onto the guanidinium carbon atom. The transfer requires low-energy side-chain rotations in **1a** to achieve conformer **1h**, which has a favorable arrangement of the C_α–H bond and the guanidine C-atom for hydrogen atom transfer (Scheme 6). The energy barrier in **TS5** (39 kJ mol^{−1} relative to **1a**; Table 3) indicates

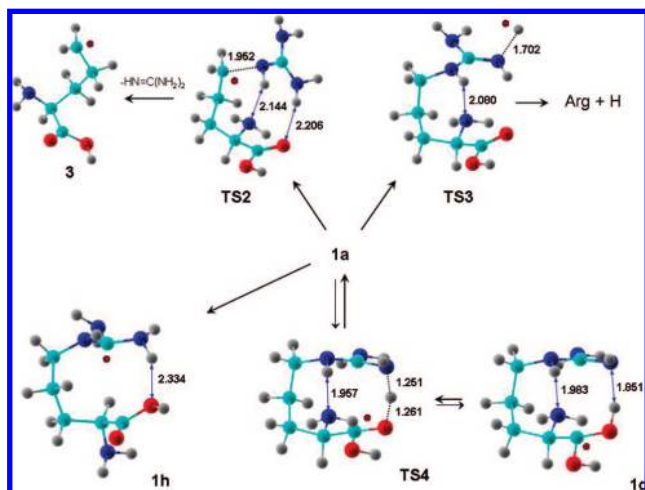
(24) DePuy, C. H.; Gronert, S.; Barlow, S. E.; Bierbaum, V. M.; Damrauer, R. *J. Am. Chem. Soc.* **1989**, *111*, 1968–1973.

Table 3. Radical Energies

species/reaction	relative energy ^{a,b}			
	B3LYP	B3-PMP2		
	6-31++G(d,p)	6-311++G(2d,p)	6-311++G(3df,2p)	aug-cc-pVTZ
1a → 1b	9	11	11 (6) ^c	
1a → 1c	12	11	10	10 (6) ^c
1a → 1d	-2	3	2	2 (-8) ^c
1a → 1e	-0.5	4	3	4 (-6.5) ^c
1a → 1f	3	6	5	5 (-5) ^c
1a → 1g	33	31	29	28
1a → 1h	8	10	9	9 (3) ^c
1a → 1i	-54	-48	-50	-51
1a → 1j	-52	-49	-49	-47
1a → 1k	20	18	18	
1a → 1l	49	75	79	78
1a → arginine + H	101	81	82	85
1a → 3 + guanidine	7	12	12	12
1a → TS1	10	12	12	12
1a → TS2	73	75	77	75
1a → TS3	95	90	90	91
1a → TS4	44	46	46	43
1a → TS5	38	41	40	39
1d → TS6	72	75	76	75
1d → TS7	96	87	86	87
3 → 4	-124	-113	-115	-115
3 → TS8	40	46	45	45
2a → 2b	15	12	12	11
2a → 2c	14	14	16	14
2a → 2d	13	13	13	13
2a → 2e	24	24	24	24
2a → 2f	-44	-44	-43	-44
2a → 2g	21	18	18	16

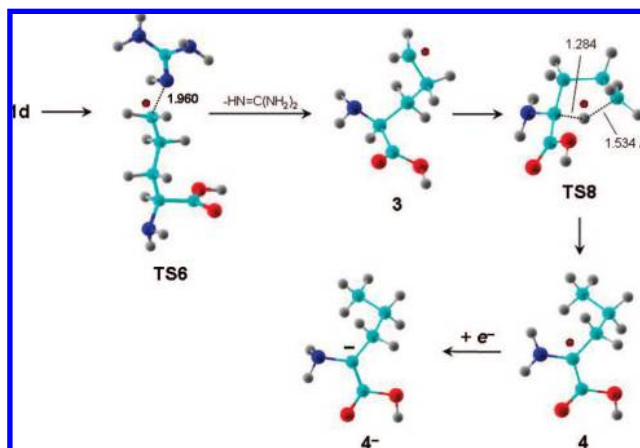
^a In units of kilojoules per mole. ^b Including B3LYP/6-31+G(d,p) or B3LYP/6-31++G(d,p) zero-point energies and enthalpies and referring to 298 K. ^c 298 K relative free energies.

Scheme 3



a fast isomerization to C_α radicals **1i** or **1j**, which are respectively 51 and 47 kJ mol⁻¹ more stable than **1a**. This reaction exothermicity reflects the difference in the dissociation energies for the C–H bond in triaminomethane (378 kJ mol⁻¹)¹ and the C_α–H bond in arginine (340 ± 10 kJ mol⁻¹).²⁵ We note that intrinsic reaction coordinate (IRC) tracing starting in **TS5** pointed to **1j** as the immediate product of H-atom migration, which also involved rotation about the C-1–C-2 bond to achieve stabilizing hydrogen bonding between the COOH and dihydroguanidine NH groups in **1j** (Scheme 6). Further side-

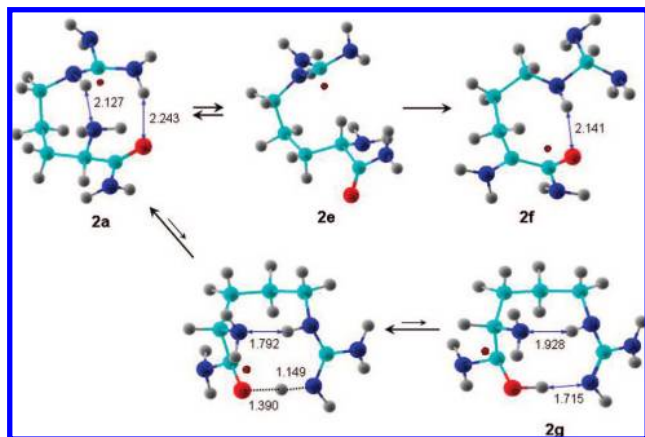
Scheme 4



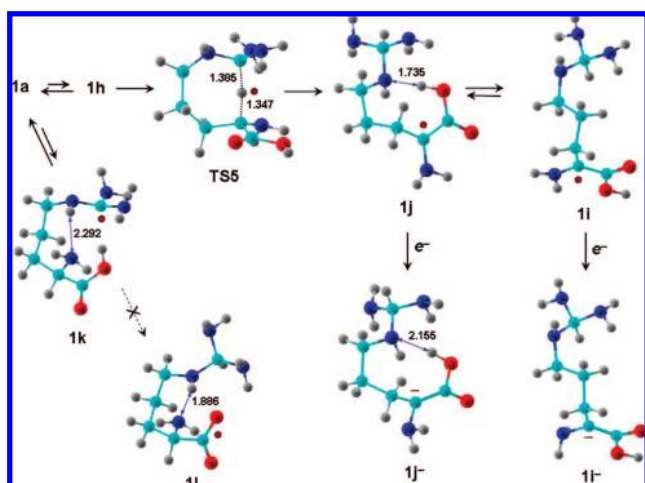
chain rotations can convert **1j** to the slightly more stable **1i** and possibly to other side-chain conformers, as well. Importantly, both **1i** and **1j** were found to have positive electron affinities: EA_{vert} = 0.47 eV and EA_{adiab} = 1.13 eV for **1i**, and EA_{vert} = 0.37 eV and EA_{adiab} = 1.03 eV for **1j** (Table 2). Since the electron affinities of **1i** and **1j** are mainly due to the stability of the C_α anions in **1i**⁻ and **1j**⁻, respectively, it is likely that the other conformers of **1i** and **1j** would also form stable anions upon electron transfer. Hence, either isomer can account for the stable anions produced upon CR. (ArgNH₂ + H)[•] radicals also showed a low energy barrier (33 kJ mol⁻¹) for the exothermic C_α–H atom migration in **2e**, forming the C_α radical **2f** (Scheme 5).⁸ The latter has a positive electron affinity (EA_{vert} = 0.57 eV, EA_{adiab} = 1.36 eV) in line with other peptide C_α

(25) Rauk, A.; Yu, D.; Taylor, J.; Shustov, G. V.; Block, D. A.; Armstrong, D. A. *Biochemistry* **1999**, *38*, 9089–9096.

Scheme 5



Scheme 6



radicals studied previously.²⁶ Thus, energetically favorable C_{α} -H atom migrations in both $(\text{Arg} + \text{H})^{\bullet}$ radicals account for the formation of stable isomers that can explain the formation of stable anions on CR.

Note that, in principle, stable anions could also be generated from isomeric arginine radicals, for example, a carboxylate (COO^{-}) from $(\text{Arg} + \text{H})$, carboximide (CONH^{-}) from $(\text{ArgNH}_2 + \text{H})$, or imide ($-\text{N}^{-}$) from either. However, the corresponding carboxyl, carboximine, and imine radicals can be safely excluded as intermediates on energy grounds. According to previous calculations and measurements, the dissociation energies of O-H bonds in carboxylic acids²⁷ and N-H bonds in amides²⁸ were 426 and 467 kJ mol^{-1} , which are both substantially greater than the C-H bond dissociation energy in the dihydroguanidyl group in **1j** and **2f**. Hence, carboxyl and carboximine radicals can be expected to be high-energy isomers of **1j** and **2f** that would not be substantially populated from **1a** and **2a**, respectively. Accordingly, a COO^{\bullet} radical (**1l**) was found to be 78 kJ mol^{-1} less stable than **1a** (Table 3). When the COO^{\bullet} group was allowed to approach the dihydroguanidine group, **1l**

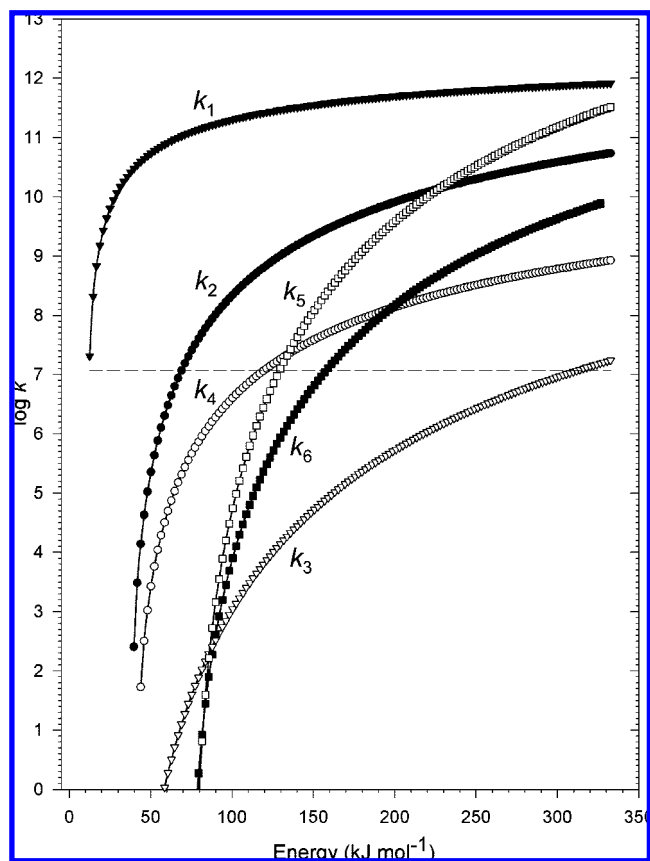


Figure 5. RRKM rate constants ($\log k, \text{s}^{-1}$) for unimolecular isomerizations and dissociations of arginine radicals on the B3-PMP2/aug-cc-pVTZ potential energy surface. The energy scale is relative to **1a**. (\blacktriangledown) k_1 for $C-C_{\beta}$ bond rotation through **TS1**; (\bullet) k_2 for C_{α} -H \rightarrow C migration in **1h** through **TS5**; (\circ) k_4 for N-H \rightarrow O migration through **TS4**; (\square) k_5 for C-N(guanidine) bond cleavage in **1a** through **TS2**; (\blacksquare) k_6 for C-N(guanidine) bond cleavage in **1d** through **TS6**; (∇) k_3 for reverse C_{α} -H \rightarrow C migration in **1j** through **TS5**. The horizontal dashed line was drawn at $\log k = 7.07$ for $k = 1/(85 \text{ ns})$, corresponding to the time scale on the Aarhus instrument.

spontaneously isomerized to **1a** by C-H \rightarrow O hydrogen atom transfer that involved another less stable conformer (**1k**, Scheme 6). Thus, C_{α} radicals **1i**, **1j**, **2f**, and their conformers are the only plausible intermediates for the formation of stable arginine anions upon CR.

RRKM Kinetic Analysis. The calculated TS energies were further used to obtain unimolecular rate constants for isomerizations and dissociations of arginine radicals (Figure 5). For the reactions to be effective on the experimental time scale ($t = 85 \text{ ns}$), the pertinent rate constants (k) must be commensurable with $1/t = 1.18 \times 10^7 \text{ s}^{-1}$, or $\log k = 7.07$. This is indicated by the dashed horizontal line in Figure 5. Internal rotations in **1a** show a fast increase of the rate constant (k_1) with the radical internal energy. At the mean E_{int} for arginine radicals produced by collisional electron transfer (137 kJ mol^{-1} , vide supra), the rotational half-life was calculated to be 2 ps, indicating that the radical conformers can undergo multiple ($\sim 10^4$) internal rotations to equilibrate on the 85 ns time scale. A corollary of this finding is that, according to the Curtin-Hammett principle,²⁹ neither the initial radical conformations nor those of their ion

(26) Hayakawa, S.; Hashimoto, M.; Matsubara, H.; Tureček, F. *J. Am. Chem. Soc.* **2007**, *129*, 7936–7949.

(27) (a) Sicilia, E.; Di Malo, P.; Russo, N. *J. Phys. Chem.* **1993**, *97*, 528–530. (b) Holmes, J. L.; Lossing, F. P.; Mayer, P. M. *J. Am. Chem. Soc.* **1991**, *113*, 9723–9728.

(28) Wood, G. P. F.; Moran, D.; Jacob, R.; Radom, L. *J. Phys. Chem. A* **2005**, *109*, 6318–6325.

(29) (a) IUPAC Compendium of Chemical Technology, 2nd ed., 1997 (<http://goldbook.iupac.org/C01480.html>). (b) Eliel, E. L. *Stereochemistry of Carbon Compounds*; McGraw-Hill: New York, 1962; pp 151–152, 237–238.

precursors should matter for the branching ratios in radical dissociations and isomerizations. Except for the side-chain rotations, the C_{α} -H atom migration is the fastest reaction of **1a** over a broad range of internal energies (k_2 , Figure 5). The rate constant for the C_{α} -H atom migration in **1a** reaches $\log k_2 = 7.07$ at an internal energy of 69 kJ mol^{-1} , indicating that a substantial fraction of **1a** having $\langle E_{\text{int}} \rangle = 137 \text{ kJ mol}^{-1}$ can isomerize to **1j**. In contrast, the reverse H-atom migration in **1j** (k_3) is slow up to $E_{\text{int}} > 300 \text{ kJ mol}^{-1}$. Thus, **1j** and its conformers can function as stable radical traps in which the radical site is located in the relatively nonreactive C_{α} position.

The $\log k$ curve for the N-H \rightarrow O migration (k_4) shows a shallow slope to reach the 7.07 limit at $E_{\text{int}} \approx 120 \text{ kJ mol}^{-1}$. Although this energy is accessible to a fraction of arginine radicals formed by collisional electron transfer, the N-H \rightarrow O migration is >50 fold slower than the C_{α} -H atom migration over the entire energy range considered in our calculations (Figure 5). In addition, at $E_{\text{int}} > 134 \text{ kJ mol}^{-1}$, the N-H \rightarrow O migration is outcompeted by the side-chain C-N bond dissociations starting from **1a** (k_5) and leading to an irreversible loss of guanidine. A similar conclusion has been reached for dissociations and isomerizations of arginine amide radicals.⁸ Hence, N-H \rightarrow O migrations appear to be kinetically ineffective in arginine radicals and indicate that the guanidinium group is a poor hydrogen-atom donor, but a good acceptor.

Loss of H from (Arg + H) $^{\bullet}$ radicals was calculated to require relatively high threshold and TS energies (e.g., **TS3**, Table 3) and has been predicted not to compete with the other unimolecular reactions.⁸ It should be noted that neutral arginine and arginine amide do not have bound anion states and cannot be detected as negative ions in $^+CR^-$ spectra. Neutral molecules can undergo dissociative ionization forming stable $(M - H)^-$ anions that may account for the m/z 173 and 172 peaks in the CR spectra. However, the high abundance of the $(M - H)^-$ ions in the 3 keV $^+CR^-$ spectra (Figure 1a) is incompatible with the calculated small fraction of H atom loss. We tentatively assign the formation of the $(M - H)^-$ ions to collision-induced dissociations (CID) of the $(M + H)^-$ ions from both arginine and arginine amide. CID of anions is also indicated by the loss of NH_3 (m/z 158) and CO_2 (m/z 131), which are typical anion dissociations.³⁰

Relevance to ECD and ETD. The arginine and arginine amide radicals under study here can be viewed as simple models for peptide radicals having Arg residues at the C-terminus (as in **1a** and **1b**), within the peptide chain (as in **2a**), and at the N-terminus (as in **2b**). The case of C-terminal arginine is most relevant for ECD and ETD of tryptic peptides. The hydrogen-bonding pattern of the guanidinium group in the precursor cations may differ for the arginine and arginine amide ions studied here on one hand, and larger arginine-containing peptide cations used in ECD and ETD, on the other. However, the present and previous calculations unambiguously indicated that hydrogen bonding to the peptide backbone of the reduced guanidinium group is substantially weakened upon electron capture in the Arg residue,⁸ allowing for fast rotations of the arginine side chain, as modeled for radicals of the **1** and **2** type and also for small Arg-containing peptides.³¹ Out of the

reactions that the reduced Arg residues can undergo, cleavage of the C-N(guanidine) bond is insensitive to the Arg side-chain conformation, as evidenced by the very similar TS energies for this dissociation in hydrogen-bonded structures **1a** and **2b** and unfolded structures **1d** and **2d** (75, 68, 75, and 70 kJ mol^{-1} , respectively). This implies that the loss of guanidine from peptide radicals on ECD and ETD should not be very sensitive to the peptide structure, in keeping with the frequently observed loss of guanidine.⁵ By contrast, rearrangements requiring tight transition states, such as C_{α} -H atom migrations to the guanidine moiety and N-H \rightarrow O migrations to the peptide backbone, are more likely to be affected by the peptide secondary structure because it may hamper access to C_{α} positions and amide groups at some amino acid residues. The fact that the H-atom affinity of the guanidinium radical group (378 kJ mol^{-1})¹ exceeds the C_{α} -H bond dissociation energies in all natural amino acid residues (326 – 358 kJ mol^{-1})²⁵ indicates that arginine radicals can function as stable radical traps in isomerizations of peptide cation radicals formed by electron capture or transfer. How efficient this trapping is and which amino acid residues are involved in it depends on the peptide backbone conformation, which has to be determined for the particular amino acid composition and sequence. Furthermore, the inverse hydrogen migration in arginine radicals is likely to compete with other rearrangements in charge-reduced peptides involving C_{α} -H bonds³² and side-chain groups.⁷

It should be noted that the Arg radical reactivity is contingent upon its formation by electron capture in the guanidinium group. The recombination energy of the latter is comparable to those of the other charged peptide groups, for example, the N-terminus and lysine ammonium³³ and the histidine imidazolium,³⁴ and thus it does not provide any clear-cut clue as to the site of electron attachment. Recent results with electron capture in fixed-charge tagged peptides indicate that the protonated Arg moiety competes for an electron with the other charged groups and amide carbonyls, and may be reduced in only a small fraction of peptide ions.³¹ This implies that the arginine effect on peptide ECD and ETD fragmentations needs to be analyzed for each particular peptide structure to achieve reliable spectra interpretation.

Conclusions

Charge inversion mass spectra of protonated arginine and arginine amide ions corroborate the theoretically predicted hydrogen atom migration from the C_{α} position to the guanidinium group in arginine and arginine amide radicals. This finding has important implications for the reactivity of peptide cation radicals produced by electron capture or transfer, where arginine residues can function as radical traps hampering backbone fragmentations. The efficiency of such arginine radical traps depends on their formation by electron capture and also on steric access to the peptide backbone, which is determined by the peptide conformation.

- (30) (a) Kulik, W.; Heerma, W. *Biomed. Environ. Mass Spectrom.* **1988**, *15*, 419–427. (b) Bertrand, M. J.; Thibault, P. *Biomed. Environ. Mass Spectrom.* **1986**, *13*, 347–355. (c) Waugh, R. J.; Bowie, J. H. *Rapid Commun. Mass Spectrom.* **1994**, *8*, 169–173.
- (31) Chamot-Rooke, J.; Malosse, C.; Frison, G.; Tureček, F. *J. Am. Soc. Mass Spectrom.* **2007**, *18*, 2146–2161.

- (32) (a) O'Connor, P. B.; Lin, C.; Courmoyer, J. J.; Pittman, J. L.; Belyayev, M.; Budnik, B. A. *J. Am. Soc. Mass Spectrom.* **2006**, *17*, 576–585. (b) Belyayev, M. A.; Courmoyer, J. J.; Lin, C.; O'Connor, P. B. *J. Am. Soc. Mass Spectrom.* **2006**, *17*, 1428–1436. (c) Jones, J. W.; Sasaki, T.; Goodlett, D. R.; Tureček, F. *J. Am. Soc. Mass Spectrom.* **2007**, *18*, 432–444.
- (33) Tureček, F.; Syrstad, E. A. *J. Am. Chem. Soc.* **2003**, *125*, 3353–3369.
- (34) Nguyen, V. Q.; Tureček, F. *J. Mass Spectrom.* **1996**, *31*, 1173–1184.

Acknowledgment. F.T. thanks the NSF for support through Grants CHE-0349595 and CHE-0750048 for experiments and CHE-0342956 for computations. Support for the Computational Chemistry Facility at the Department of Chemistry has been jointly provided by the NSF and University of Washington. F.T. also thanks the University of Aarhus Department of Physics and Astronomy for the Visiting Professor Fellowship in June–August 2007. S.B.N. thanks the Danish Natural Science Research Council (Grants 21-04-0514 and 272-06-0427), Carlsbergfondet (Grant 2006-01-0229),

and Lundbeckfonden for support. S.H. thanks the Osaka Prefecture University for support by Special Research Grant in 2007.

Supporting Information Available: Schemes S1 and S2, complete ref 12, and Tables S1–S38 of optimized structures in Cartesian coordinate format. This information is available free of charge via the Internet at www.pubs.acs.org.

JA800207X